Electronic Supplementary Material (ESI) for Physical Chemistry Chemical Physics.


# Electron-level insight into efficient synergistic oxygen evolution catalysis at multimetallic sites in PtNiFeCoCu high-entropy alloys

Sen Ming[a], Kun Meng[a,*], Chengyi Hou[a], Lei Qin[a], Shitao Wang[a]，Ju Rong[a], Xiaohua Yu[a], Hongying Hou[a,*]

[a]Faculty of Materials Science and Engineering, Kunming University of Science and Technology, Kunming, 650093, China.

**E-mail addresses:** mkkmust@163.com, hongyinghou@kust.edu.cn

**Table S1.** A summary of HEA electrocatalysts with favorable OER catalytic activity

| Catalysts | Catalytic reaction | Reference |
|---|---|---|
| CoCrFeMnNi–P | HER、OER | [1] |
| CoFeLaNiPt | HER、OER | [2] |
| AlNiCoFeX (X = Mo, Nb, Cr) | ORR、OER | [3] |
| NiCoFeMoMn | HER、OER | [4] |
| PtRuFeCoNi | ORR、OER | [5] |
| FeCoNiCuMn | HER、OER | [6] |

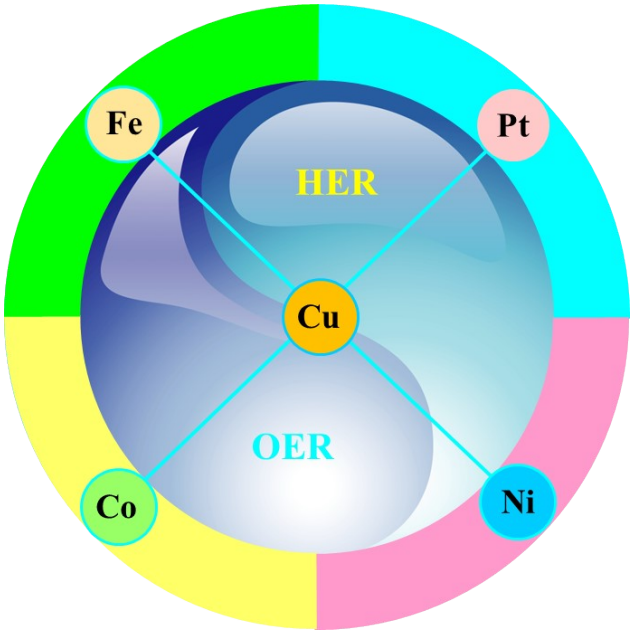


**Figure S1.** HEA Composition Schematic.

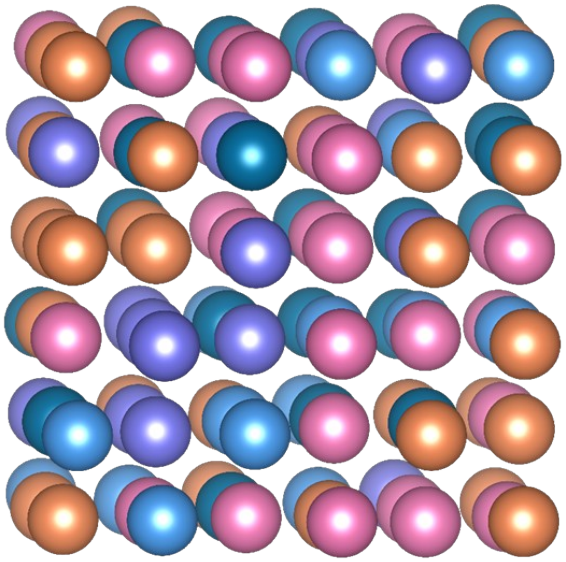

**Figure S2.** Optimized geometries of the PtNiFeCoCu HEA structure.

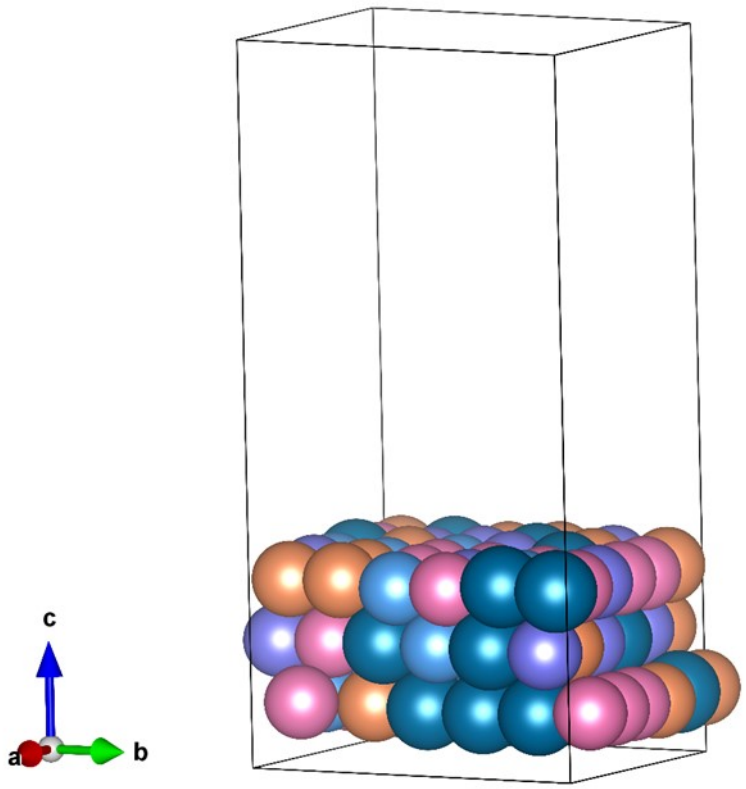


**Figure S3.** Chemical structure model of the PtNiFeCoCu HEA (111) surface.

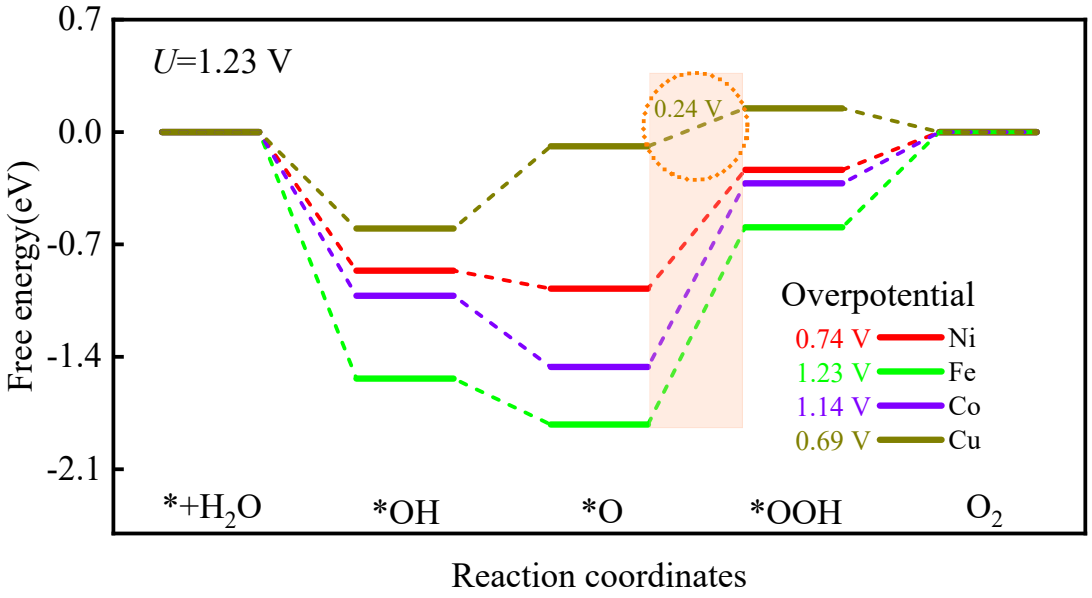


**Figure S4** Free energy landscape of the four metal sites of HEA (001) at equilibrium potential (U = 1.23 V).

**Table S2.** Charge contribution of individual metal sites during co-adsorption and the charge acquired by *O from the substrate.

| P-1 | Bader/e | P-2 | Bader/e |
|---|---|---|---|
| $Ni_{22}$ | -0.18 | $Cu_{19}$ | -0.21 |
| $Ni_{13}$ | -0.17 | $Fe_{4}$ | -0.64 |
| $Fe_{12}$ | -0.52 | $Fe_{7}$ | -0.65 |
| O | 0.89 | O | 0.93 |

***Calculation of HER energetics***

The total hydrogen evolution reaction can be written

$$H^+ + e^- \rightarrow \frac{1}{2}H_2 \quad (1)$$

It takes place at an electrode supplying the electrons, and providing an intermediate state of the process:

$$H^+ + e^- + * \rightarrow H^* \quad (2)$$

$$2H^* \rightarrow H_2 \quad (3)$$

Where the * denotes a site on the surface (so an * by itself denotes a free site and H* denotes a hydrogen atom adsorbed on the surface).

The free energies for hydrogen adsorption ($\Delta G_{H^*}$) are calculated from the Eq. 4:

$$\Delta G_{H^*} = \Delta E_{H^*} + \Delta ZPE - T\Delta S \quad (4)$$

Where the $\Delta E_{H^*}$, $\Delta ZPE$, $T$ and $\Delta S$ represent the binding energy, zeropoint energy change, temperature and entropy change of H adsorption system, respectively.

The vibration entropy is H at the adsorbed states is negligible. Thus, $\Delta S$ can be obtained from the following Eq. 5:

$$\Delta S = S_{H^*} - \frac{1}{2}S_{H_2} \approx -\frac{1}{2}S_{H_2} \quad (5)$$

Where $S_{H_2}$ is the entropy of $H_2$ in the gas phase at the standard conditions.

Besides, $\Delta ZPE$ can be calculated from the Eq. 6:

$$\Delta ZPE = ZPE_{H^*} - \frac{1}{2}ZPE_{H_2} \quad (6)$$

Thus, the free energy of the adsorbed state can be calculated using the simplified Eq. 7[7]:

$$\Delta G_{H^*} = \Delta E_{H^*} + 0.24eV \quad (7)$$

As illustrated in Figure S5, we randomly selected eight potential sites on the PtNiFeCoCu HEA (111) surface and calculated their $\Delta G_{H^*}$ values. $\Delta G_{H^*}$ is a key descriptor for evaluating the HER performance of electrocatalysts. As can be seen from the figure, the $\Delta G_{H^*}$ values of these eight active sites are all relatively low (around 0.3 eV). This indicates that the PtNiFeCoCu HEA (111) exhibits notable HER performance under acidic conditions. In addition, there is a significant synergistic effect at multiple sites in the second step of H* adsorption/$H_2$ desorption (Heyrovsky step).

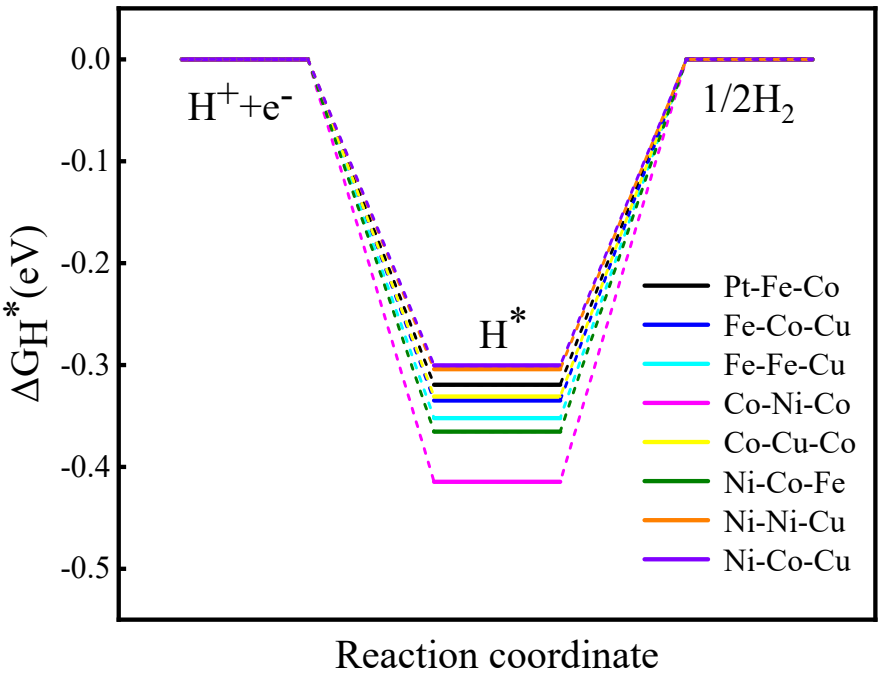


**Figure S5** Free energy ($\Delta G_{H^*}$) diagram for HER at different catalytic sites on the PtNiFeCoCu HEA (111) surface at U=0, pH=0.

## References

[1] Zhao X, Xue Z, Chen W, et al. Eutectic synthesis of high-entropy metal phosphides for electrocatalytic water splitting[J]. ChemSusChem, 2020, 13(8): 2038-2042.

[2] Glasscott M W, Pendergast A D, Goines S, et al. Electrosynthesis of high-entropy metallic glass nanoparticles for designer, multi-functional electrocatalysis[J]. Nature Communications, 2019, 10(1): 2650.

[3] Fang G, Gao J, Lv J, et al. Multi-component nanoporous alloy/(oxy) hydroxide for bifunctional oxygen electrocatalysis and rechargeable Zn-air batteries[J]. Applied Catalysis B: Environmental, 2020, 268: 118431.

[4] Liu H, Qin H, Kang J, et al. A freestanding nanoporous NiCoFeMoMn high-entropy alloy as an efficient electrocatalyst for rapid water splitting[J]. Chemical Engineering Journal, 2022, 435: 134898.

[5] Zhang P, Hui X, Nie Y, et al. New Conceptual Catalyst on Spatial High-Entropy Alloy Heterostructures for High-Performance Li-O2 Batteries[J]. Small, 2023, 19(15): 2206742.

[6] Zhu H, Sun S, Hao J, et al. A high-entropy atomic environment converts inactive to active sites for electrocatalysis[J]. Energy & Environmental Science, 2023, 16(2): 619-628.

[7] Nørskov J K, Bligaard T, Logadottir A, et al. Trends in the exchange current for hydrogen evolution[J]. Journal of The Electrochemical Society, 2005, 152(3): J23.